

Monitoring Al-Razzaza Lake and its Surrounding Areas Using Remote Sensing and GIS

Tabarak H. Mohammed Hussain^{1*} and Ban A. Abbas²

¹Department of Remote Sensing & GIS, College of Science, University of Baghdad, Baghdad, Iraq

²Remote Sensing Unit, College of Science, University of Baghdad, Baghdad, Iraq

*Corresponding author: Tabarak.Ali2309@sc.uobaghdad.edu.iq

Abstract

Al-Razzaza Lake is one of the most important water resources in Iraq, holding significant economic and environmental value for the country. The lake is now undergoing significant ecological changes and experiencing water level declines, primarily driven by increased evaporation due to climate change and reduced inflow from the Euphrates River. It is, therefore, important to monitor the changes affecting the lake using remote sensing and geographic information systems (GIS). This study aims to assess environmental changes in Al-Razzaza Lake by analyzing Landsat 4-5 images for 2004 and Landsat 8-9 images for 2014 and 2024. Climate data were obtained from the NASA Energy website (2004 and 2014) and the Al-Razzaza station of the Ministry of Agriculture (2024). Supervised classification using the Maximum Likelihood method and the Normalized Difference Water Index (NDWI) was applied to classify the study area into water, soil, and vegetation. The classification achieved overall accuracies of 94%, 97%, and 98% for 2004, 2014, and 2024, respectively. The results indicated that the water surface area declined significantly from 549.22 km² in 2004 to 189.77 km² in 2024, accompanied by an expansion in the soil area and a reduction in vegetation cover. A strong inverse correlation ($r = -0.98$) was observed between high temperatures and declining water surface areas, while a positive correlation ($r = 0.98$) was found between rainfall and water surface areas. The study features the alarming degradation of Al-Razzaza Lake and the urgent need for continuous monitoring and adaptive water resource management strategies.

Article Info.

Keywords:

Classification, Supervised classification, Unsupervised classification, GIS, Maximum likelihood Classification.

Article history:

Received: Jan. 16, 2025

Revised: May 20, 2025

Accepted: May 21, 2025

Published: Mar. 01, 2026

1. Introduction

Al-Razzaza Lake, the second largest lake in Iraq, lies within a wide valley that also includes Bahr Najaf and the lakes of Habbaniyah and Tharthar. Like many other inland water bodies across the country, Al-Razzaza has undergone severe environmental degradation—particularly since 2003. Factors contributing to this decline include climate change, increasing temperatures, and reduced inflow from the Euphrates River, mainly due to dam constructions in Syria and Turkey [1,2]. If these stressors persist or intensify, the need for consistent monitoring of the lake's condition, especially its water levels and vegetative cover, becomes more urgent. Issues, like drought, shifting landforms, and climate variability have moved from abstract concerns to immediate environmental challenges. These factors directly impact water availability, agricultural planning, and the resilience of already vulnerable ecosystems. Meeting such complex challenges calls for monitoring approaches that are both broad in scope and consistent over time, something traditional field methods struggle to achieve. In this context, remote sensing technologies and geographic information systems (GIS) have become essential tools. They support large-scale environmental monitoring by enabling the detection of floods, droughts, and geomorphological shifts and by assisting in the management of natural resources, including land, soil, forests, and inland water bodies. GIS and satellite-based surveying allow reliable temporal and spatial mapping of environmental systems, forming a critical basis for informed decision-making [3,4]. One of the core capabilities of GIS lies in

tracking changes across time. Comparing aerial or satellite imagery from different periods is a standard technique for identifying landscape changes [5,6]. Change detection involves identifying variations in the state or condition of physical features by observing them at multiple time points, and multi-temporal data analysis makes it possible to detect both gradual trends and sudden shifts [7].

Although remote sensing offers a powerful means of capturing spatial data at large scales, the interpretation of that data can still be influenced by observer subjectivity [8,9]. This makes image processing techniques, as well as the integration of remote sensing data with supporting datasets (e.g., ground truth observations, topographic and land use maps), crucial for obtaining reliable and objective environmental assessments. GIS plays a central role in managing, combining, and analyzing such data, offering a practical framework for monitoring surface water dynamics, especially in vulnerable systems like Al-Razzaza Lake [10,11].

Image classification is a foundational step in extracting meaningful patterns from remote sensing data. By assigning each pixel or image segment to a land cover category based on its spectral and spatial characteristics, classification algorithms allow researchers to quantify environmental features, such as vegetation, soil, and water [12,13].

This study used advanced classification techniques and the normalized difference water index (NDWI) to evaluate the impact of long-term environmental changes on Al-Razzaza Lake. Satellite images from 2004, 2014, and 2024 were analyzed to support more sustainable water and land management efforts in the region. Two principal classification strategies were used in the analysis: supervised and unsupervised classification.

1.1. Supervised Classification

Supervised classification depends on training samples that represent predefined land cover categories. These samples are manually selected based on user knowledge, prior field data, or visual interpretation. While this method benefits from human expertise, it remains sensitive to subjective judgment. Limited or inaccurately labelled training data can reduce classification accuracy and compromise the generalizability of results [14].

1.2. Unsupervised Classification

Unsupervised classification, often referred to as clustering, relies entirely on the statistical characteristics of the image. It groups pixels into classes based on their spectral similarities without prior knowledge or external reference data [15]. Common algorithms include ISODATA and k-means for unsupervised approaches, while maximum likelihood and minimum distance are frequently used in supervised contexts [16].

In this study, maximum likelihood classification was selected due to its improved performance in delineating land cover types.

1.3. Supervised Maximum Likelihood Classification

The maximum likelihood method is among the most widely adopted classification algorithms in remote sensing, primarily due to its probabilistic foundation and effectiveness across diverse landscapes. It assumes that the distribution of spectral values within each class follows a normal (Gaussian) distribution. The process begins with the delineation of training regions for each class. These are used to estimate the statistical parameters of the class distributions. Each pixel is then evaluated based on the likelihood that it belongs to a given class and is assigned to the one with the highest probability [17-19].

1.4. Classification Accuracy Assessment

Accuracy assessment is an integral step in evaluating the reliability of classification outputs. It quantifies the degree to which the classified map agrees with reference data, thus providing a measure of confidence in the results. Since remote sensing-based classifications are prone to errors due to misclassified pixels or spectral overlap, independent validation using appropriate accuracy metrics is essential [20]. One commonly used measure of agreement beyond chance is the kappa statistic, which evaluates consistency between classifiers, raters, or diagnostic procedures. It is often considered a measure of precision in classification performance [21,22]. The kappa coefficient (K) is calculated using Eq. (1).

$$K = (P_a - P_c)/(1 - P_c) \quad (1)$$

Where $P_a = (a + d)/N$, (a, d) is the number of correctly classified instances in the main diagonal of the confusion matrix, N is the number of correctly classified instances in the main diagonal of the confusion matrix, and P_c is the expected agreement by chance. The kappa coefficient ranges from -1 to +1. A value close to +1 indicates complete agreement between the classification result and the reference data. In contrast, a value near -1 reflects very poor agreement, suggesting that the classification is performing worse than random chance [23].

1.5. Correlation Coefficient

Pearson's product-moment correlation coefficient (r) is the most widely used measure of the relationship between two variables, which may be continuous or dichotomous. A value of -1 indicates a perfect negative linear relationship, while a value of +1 indicates a perfect positive linear relationship. It is well established that correlation does not indicate causation [21,24,25].

1.6. NDWI

McFeeters introduced the NDWI in 1996 to identify surface water in wetland areas and to estimate the extent of surface water bodies [26]. NDWI values range from -1 to +1, with water bodies typically showing values greater than 0.5 [27]. The index is calculated using Eq. (2).

$$NDWI = (Green - NIR)/(Green + NIR) \quad (2)$$

where Green is a green band and NIR is a near-infrared band.

2. Study Area

Part of the Western Plateau, AL-Razzaza Lake, was created in 1969 to protect the southern regions from heavy rains. It is known for its semi-arid climate, which is hot in the summer and cold in the winter. The study area is between longitude ($43^{\circ} 05' 00''$ - $44^{\circ} 10' 00''$) east and latitude ($32^{\circ} 27' 00''$ - $34^{\circ} 00' 00''$) north (Fig. 1). Locally, the lower portion of the lake is within the Karbala Governorate, while the upper portion is within the Anbar Governorate. The lake serves as a reservoir that supplies up to 25.75 billion cubic meters of floodwater for storage across an 1810 square kilometre surface area.

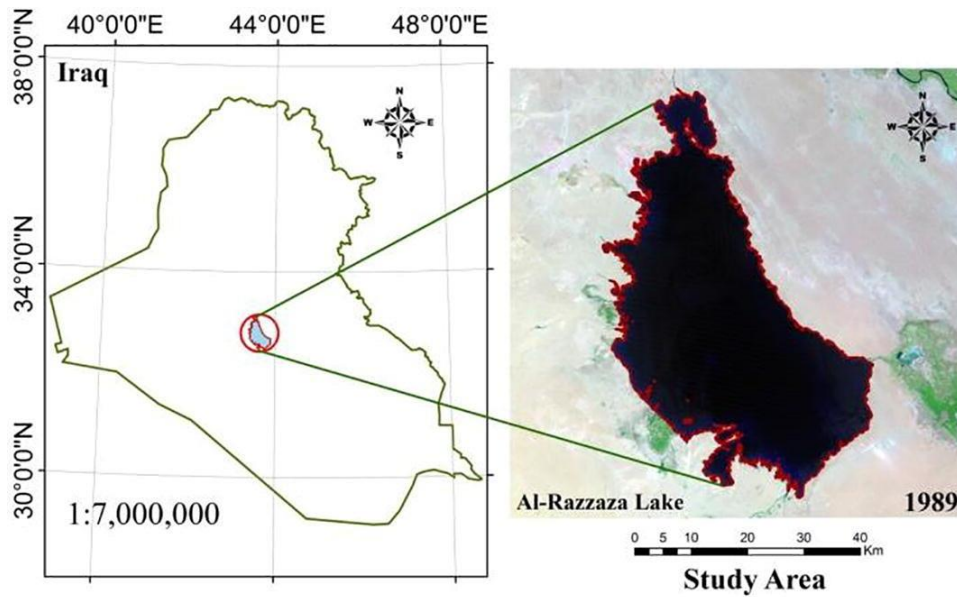


Figure 1: The study area of AL-Razzaza Lake in Iraq. Reused with permission from Jumaah et al. [28].

3. Methodology

After downloading Landsat (8-9) satellite images for 2014 and 2024 and Landsat (4-5) images for 2004 (due to the absence of Landsat 8-9 of 2004), images were selected for October to reduce seasonal bias, i.e. their clarity and freedom from clouds or any other effects. To ensure comparability, atmospheric correction was applied to all images, and spatial resampling was performed to harmonize resolution across sensors.

A composite band was created using bands (4, 3, 2) for Landsat 8-9 and (3, 2, 1) for Landsat 4-5, corresponding to red, green, and blue wavelengths in each sensor. This arrangement produced true-color images that reflect natural human perception and facilitate a more intuitive interpretation of land cover. These combinations are widely accepted in environmental monitoring for distinguishing between water, vegetation, and built-up surfaces [26,27].

Image preprocessing, band composition, and masking were performed using ArcGIS. The study area mask was digitized based on the lake's known geographic extent using satellite basemaps, ensuring uniform boundaries across all time points. The resulting pre-processed images for 2004, 2014, and 2024 are shown in Figs. 2-4, and served as inputs for a supervised classification step using the Maximum Likelihood algorithm, described in the next section.

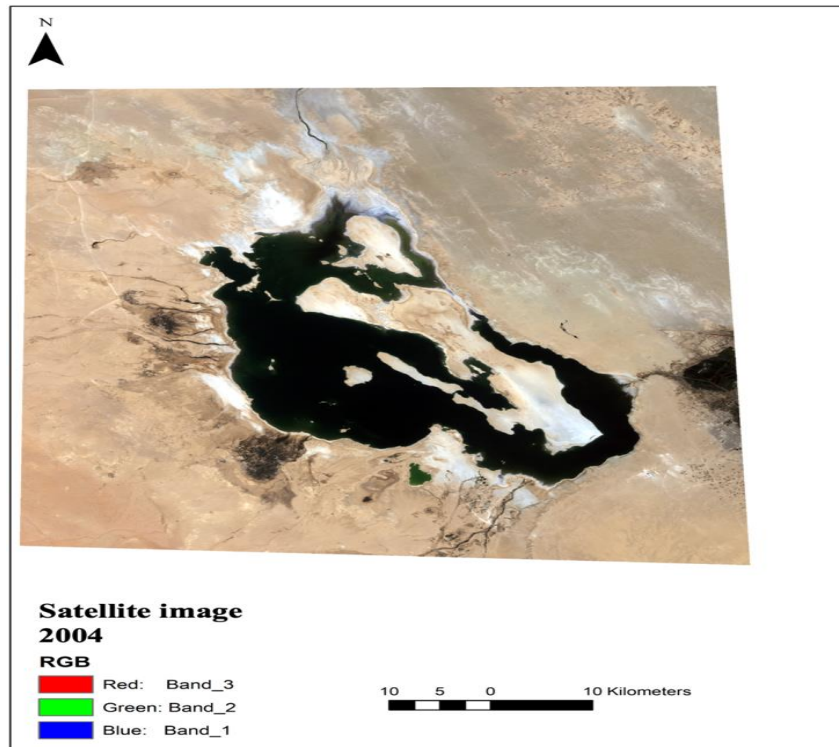


Figure 2: The study area after composite band and clipping (2004).

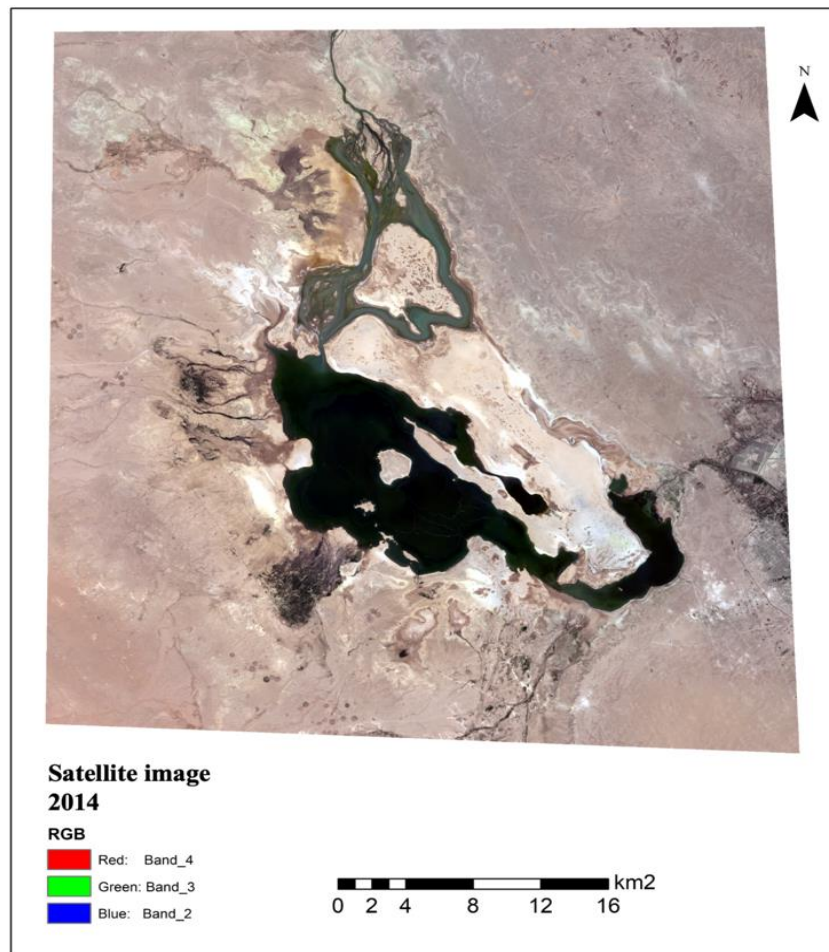


Figure 3: The study area after composite band and clipping (2014).

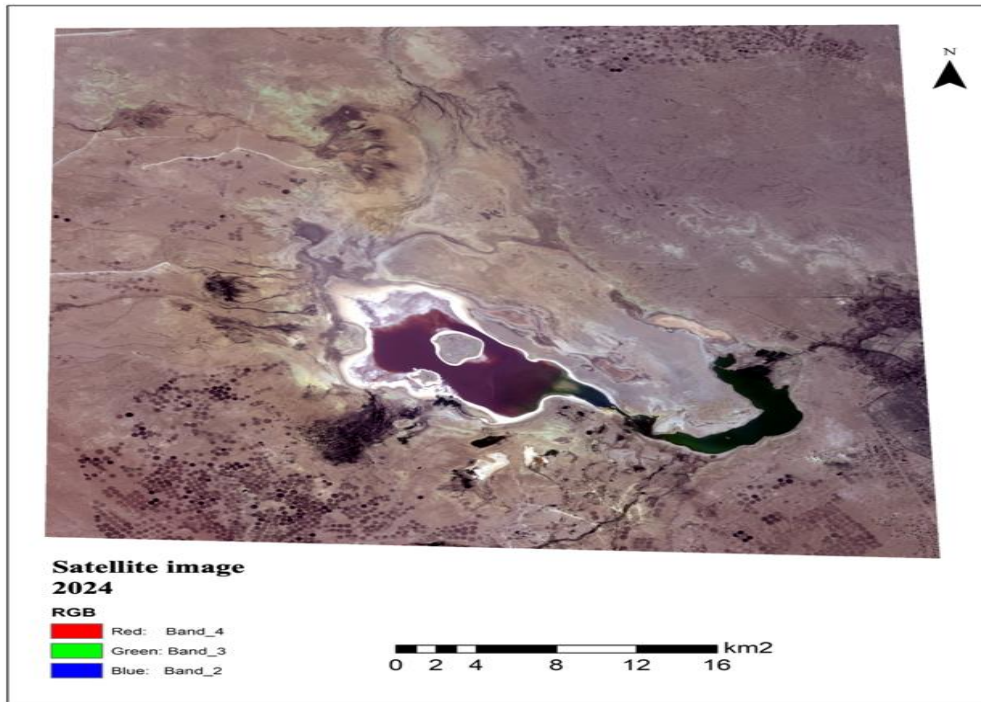


Figure 4: The study area after composite band and clipping (2024).

4. Results and Discussion

To obtain accurate results, supervised classification was carried out using the maximum likelihood method. Samples were taken for three land cover categories: soil, water, and vegetation, based on training regions identified in the images, i.e. Samples taken from images. The classified outputs for each year are shown in Figs. 5-7.

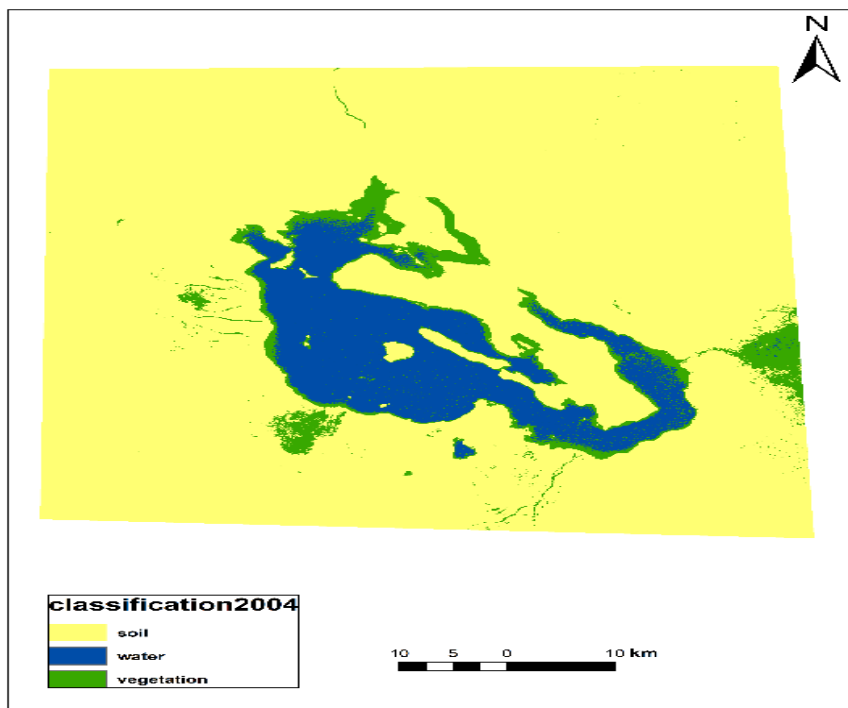


Figure 5: Study area post-classification for 2004.

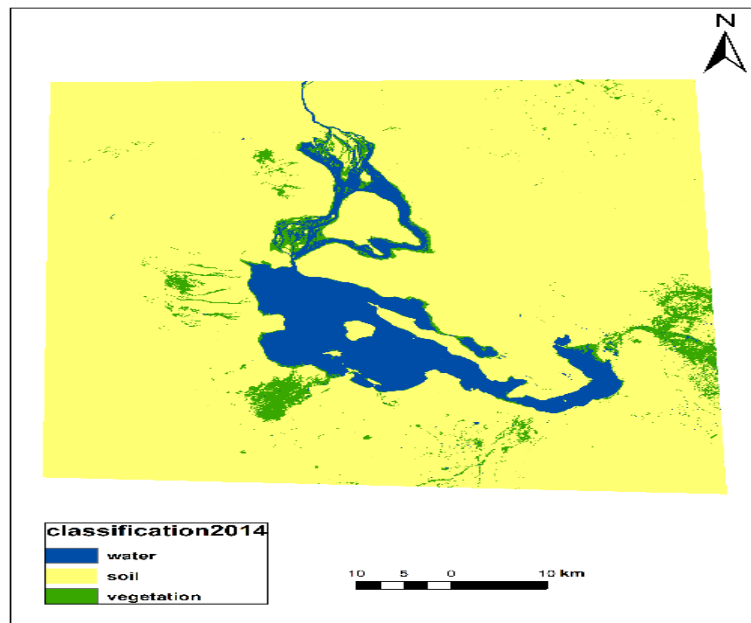


Figure 6: Study area post-classification for 2014.

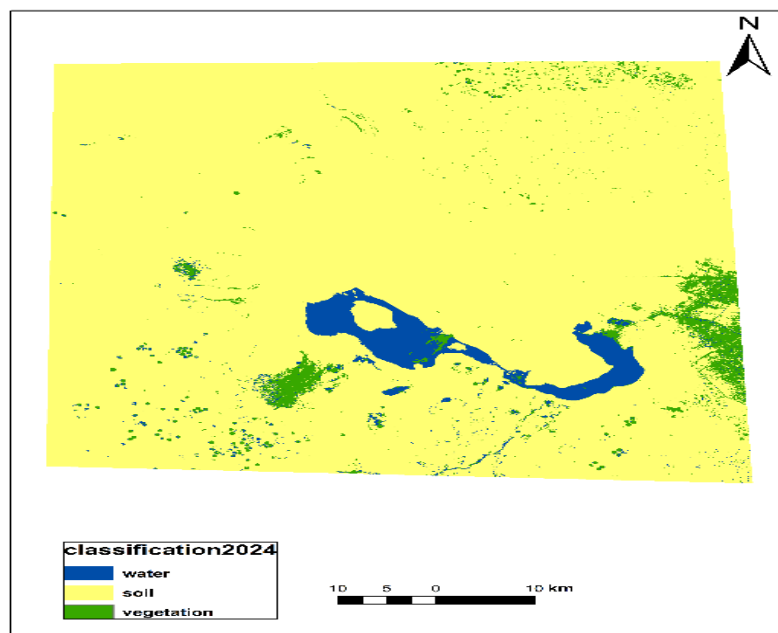


Figure 7: Study area post-classification for 2024.

After classification, the raster images were converted to vector (polygon) format. The area in square kilometres was then calculated for each polygon. Using the frequency tool in the processing toolbox, similar polygons were grouped by class, allowing each group to represent one of the three defined categories. Table 1 presents the classified area coverage of water, soil, and vegetation for 2004, 2014, and 2024. These results reflect the spatial distribution and temporal dynamics of land cover classes within the Al-Razzaza Lake region based on supervised classification results.

It is evident that a noticeable decline in surface water has occurred over the 20 years. Water coverage decreased from 549.22 km² in 2004 to just 189.77 km² in 2024, representing a 65.5% reduction. This shrinkage coincides with a steady increase in soil

area, which expanded from 4297.23 km² to 4747.88 km². Similarly, vegetation cover decreased from 266.03 km² in 2004 to 174.81 km² in 2024, which presents the stress on the surrounding ecosystems (Table 1 and Fig. 8). The frequency and grid code values further confirm the consistency of classification across the years, with each class reliably mapped and aggregated.

Table 1: Frequency, grid code, and surface area for water, soil, and vegetation in the study area.

Year	FID	Name	Frequency	Grid Code	Area (Km ²)
2004	1	Water	3892	13	549.22
	2	Soil	878	1	4297.23
	3	Vegetation	13290	22	266.03
2014	1	Water	2390	1	455.61
	2	Soil	2893	15	4440.9
	3	Vegetation	8770	32	215.93
2024	1	Water	7686	1	189.77
	2	Soil	3103	18	4747.88
	3	Vegetation	11736	37	174.81

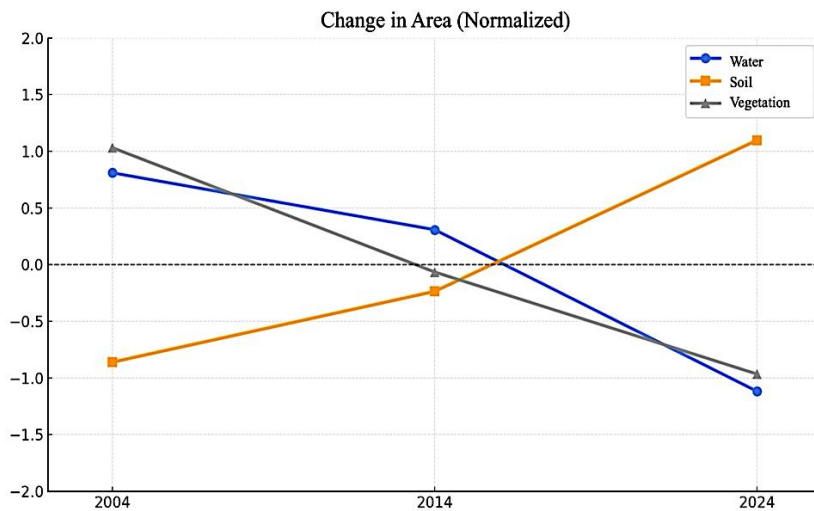


Figure 8: The change in the areas of water, vegetation, and soil of the lake during 2004, 2014, and 2024.

The classification accuracy was evaluated using supervised classification results from the Maximum Likelihood method. Object-based image analysis was conducted in ArcGIS Pro to generate a segmented shapefile, within which 150 stratified random points were distributed across the three land cover categories: water, soil, and vegetation. Each point was manually cross-checked against high-resolution reference imagery obtained from the USGS Earth Explorer, serving as the ground truth dataset. A confusion matrix was generated for each year (2004, 2014, and 2024) to compare the classified outputs with the ground truth. Accuracy metrics, including overall accuracy and the Kappa coefficient, were calculated in Microsoft Excel to ensure full traceability.

The classification for 2004 achieved an overall accuracy of 94% and a Kappa coefficient of 0.84, which suggests strong agreement between the classification and the reference data (Table 2). While soil and water classes were classified with high precision, six vegetation pixels were misclassified as water, reflecting moderate confusion between these two classes. The 2014 classification improved to an overall accuracy of 97% with a Kappa coefficient of 0.88 (Table 3). The matrix shows excellent class separation,

particularly for soil and water categories, with minimal misclassification. For 2024, overall accuracy reached 98%, and the Kappa coefficient was 0.85, further confirming the robustness of the classification (Table 4). Minor misclassifications occurred between water and soil, but their impact on overall reliability was negligible. Collectively, these results support the validity of the classification approach and provide a solid foundation for subsequent area calculations and environmental analyses.

Table 2: The accuracy classification assessment for 2004.

		Reference			Row Total
		Soil	Water	Vegetation	
Classification	Soil	77	0	0	77
	Water	0	15	0	15
	Vegetation	0	6	2	8
Column Total		77	21	2	100
Overall Classification Accuracy (%)		94.00%			
Kappa Coefficient		0.84			
P _a		0.94			
P _r		0.626			

Table 3: The accuracy classification assessment for 2014.

		Reference			Row Total
		Water	Soil	Vegetation	
Classification	Water	10	0	0	10
	Soil	0	85	0	85
	Vegetation	0	3	2	5
Column Total		10	88	2	100
Overall Classification Accuracy (%)		97.00%			
Kappa Coefficient		0.88			
P _a		0.97			
P _r		0.759			

Table 4: The accuracy classification assessment for 2024.

		Reference			Row Total
		Water	Soil	Vegetation	
Classification	Water	4	1	0	5
	Soil	0	92	0	92
	Vegetation	0	1	2	3
Column Total		4	94	2	100
Overall Classification Accuracy (%)		98.00%			
Kappa Coefficient		0.85			
P _a		0.98			
P _r		0.8674			

To improve the delineation of surface water and correct the misclassification of shallow lake edges as vegetation, the NDWI was calculated according to Eq. (2), following the method introduced by McFeeters (1996) [26]. The calculation used the green and near-infrared bands (Band 3 and Band 5 for Landsat 8-9, and Band 2 and Band 4 for Landsat 4-5) reflecting standard practice for isolating water features from other land cover types. A threshold value of 0.5 was applied to classify water and non-water areas based on values commonly reported in the literature and further validated through visual inspection of known water zones within the study area. This step was particularly important, as the initial classification showed that portions of shallow water along the lake's margins were incorrectly identified as vegetation. Applying NDWI allowed a more

accurate assessment of the water surface extent and improved the overall interpretation of hydrological changes. Figs. 9-11 illustrate the NDWI-derived water classifications for the years 2004, 2014, and 2024, respectively, and highlight changes in the spatial extent of Al-Razzaza Lake over the study period.

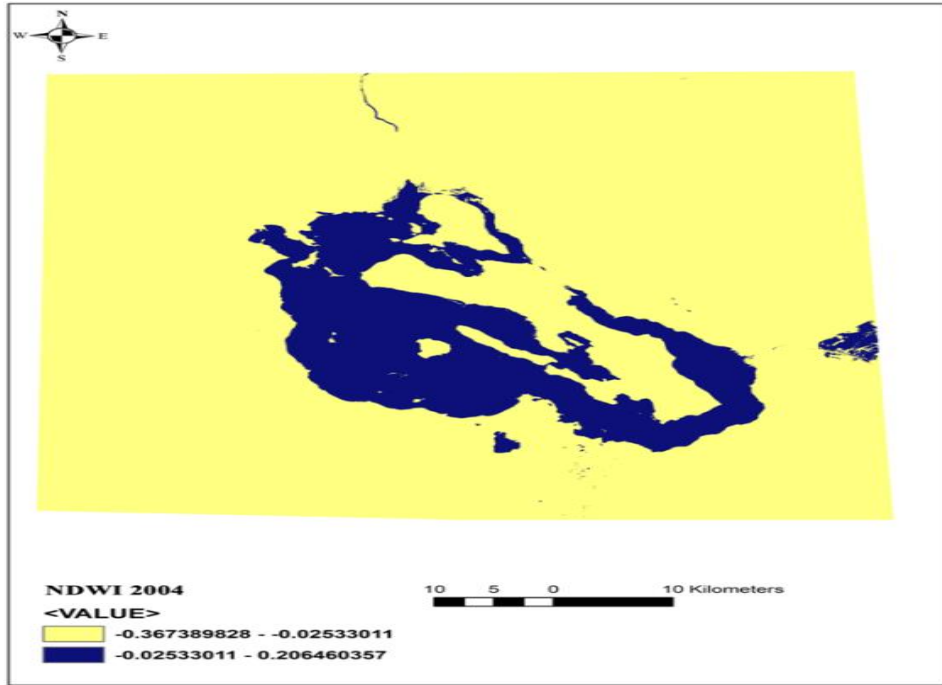


Figure 9: NDWI output for Al-Razzaza Lake in 2004.

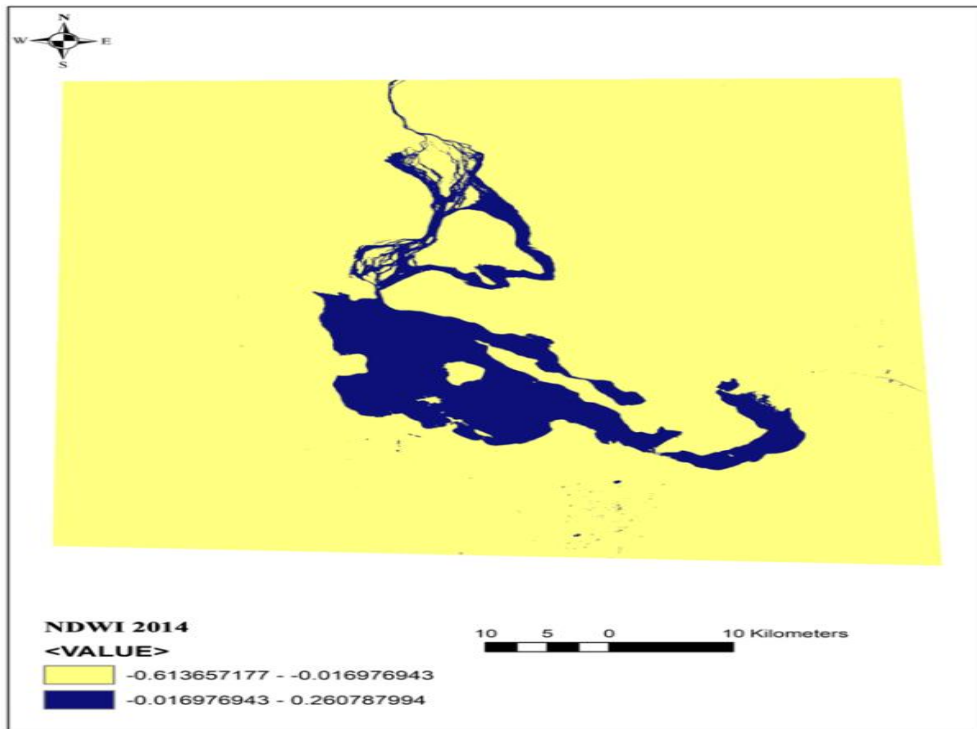


Figure 10: NDWI output for Al-Razzaza Lake in 2014.

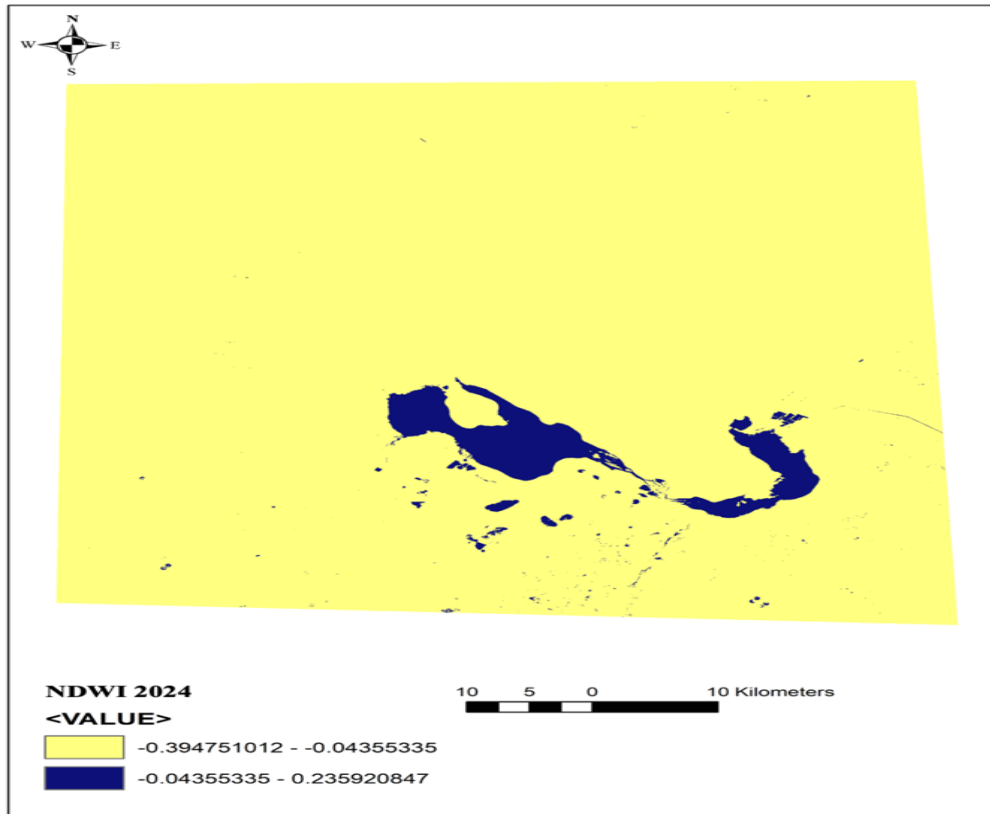


Figure 11: NDWI output for Al-Razzaza Lake in 2024.

Following the application of NDWI, surface water areas were extracted and quantified for 2004, 2014, and 2024. As shown in Table 5, the surface water area of Al-Razzaza Lake declined markedly, from 742.08 km² in 2004 to 470.73 km² in 2014, and then to 167.23 km² in 2024. The trend reflects a significant reduction in surface water extent over the two-decade period.

To understand the influence of climate variables on lake surface area, a Pearson correlation coefficient was calculated between the extracted water areas and the average annual temperatures for the same years. Table 6 presents the results, indicating a strong inverse correlation ($r = -0.98$). Higher temperatures were associated with smaller lake surface areas, while lower temperatures coincided with larger extents.

In addition, the correlation between average annual precipitation and surface water area was examined. As indicated in Table 7, a positive correlation coefficient ($r = 0.98$) was observed. Greater rainfall was linked to increased surface water area, whereas lower rainfall values corresponded with reduced lake coverage. The findings suggest that the surface water dynamics of Al-Razzaza Lake are highly responsive to changes in temperature and precipitation levels.

Table 5: NDWI-extracted surface water area (km²) within the study area.

Year	FID	Frequency	Grid Code	Area (Km ²)	Name
2004	1	632	2	742.08	Water
2014	1	651	2	470.73	Water
2024	1	881	2	167.23	Water

Table 6: Correlation coefficient between annual average and the water surface area of Al-Razzaza Lake.

Year	Avg. T (°C)	Area (Km ²)	r
2004	11.6	549.22	-0.98
2014	12.65	455.61	
2024	26.2	189.77	

Table 7: Correlation coefficient between the annual average rainfall rate and the water surface area of Al-Razzaza Lake.

Year	Avg. precipitation (mm/year)	Area (Km ²)	r
2004	5.93	549.22	0.98
2014	5.71	455.61	
2024	0.33	189.77	

A comparison between the classified results and NDWI-derived outputs revealed notable differences in the estimated water surface area. In 2004, the classification result identified 549.22 km² of surface water, whereas the NDWI-based extraction reported a higher value of 742.08 km². A similar pattern was observed in 2014, with a classified water area estimated at 455.61 km², compared to 470.73 km² from the NDWI. Conversely, in 2024, NDWI yielded a slightly lower estimate (167.23 km²) than the classification result (189.77 km²). These differences reflect the NDWI's ability to detect shallow and spectrally mixed water zones, particularly along the lake margins, which are often misclassified as vegetation in conventional approaches. While the supervised classification provided a general representation of land cover types, the NDWI offered enhanced precision in outlining open water by controlling the spectral contrast between green and near-infrared bands. Integrating both methods improved the reliability of the surface water assessment and provided a more comprehensive understanding of temporal changes, especially under the environmental changes affecting Al-Razzaza Lake.

Similar approaches based on Landsat images and classification techniques reported a surface water reduction of more than 80% over three decades, with lake area estimates decreasing from over 1600 km² in 1989 to fewer than 260 km² in 2019 [28]. More recent assessments using similar methods observed surface water shrinking from approximately 1450 km² in 1998 to just 370 km² by 2018 [29].

Several studies employed NDWI alongside other spectral indices, confirming its usefulness in outlining open water, especially in regions with shallow or mixed land-water boundaries [29,30]. Interestingly, assessments that relied on maximum likelihood classification and multi-class land cover mapping reported similar transitions from water to exposed soil along the lake's periphery, corresponding to findings in the current classification outputs [31]. Hydrological measurements conducted in parallel with remote sensing studies recorded declining lake elevation and volume between 2006 and 2020 and increased salinity due to high evaporation and limited recharge [2]. These observations further substantiate the interpretation that evaporation, upstream regulation, and insufficient inflow collectively contribute to Al-Razzaza Lake desiccation, a conclusion supported by the temporal patterns identified in the present analysis.

5. Conclusions

The results show a steady decline in the surface water area of Al-Razzaza Lake over the study period. The water area decreased from 549.22 km² in 2004 to 455.61 km² in 2014 and 189.77 km² in 2024. At the same time, the area of soil expanded from 4297.23 km² to 4747.88 km², and the area of vegetation cover declined from 266.03 km² to 174.81 km². Several factors may have contributed to these changes. The lake is located in a dry region where summers are scorching and rainfall is generally low. These conditions may

have increased evaporation and reduced water levels. Human activity also plays a role, including agricultural expansion, poor water planning, and reduced inflow due to dam construction upstream. The statistical analysis supports these observations. A strong inverse Pearson correlation ($r = -0.98$) was found between temperature and water area, indicating that higher temperatures were associated with smaller lake sizes. A positive correlation ($r = 0.98$) was found between rainfall and the water area, suggesting that years with more rain were also years when the lake surface was larger. Taken together, the findings suggest that both climate conditions and local human activity are influencing the ongoing shrinkage of Al-Razzaza Lake. Continuous monitoring and improved water management are necessary to protect the lake and its surrounding areas.

Acknowledgments

The authors would like to thank the Department of Remote Sensing & GIS, as well as the Remote Sensing Unit at the University of Baghdad, for their valuable support and assistance throughout this study.

Conflict of Interest

The authors declare no conflict of interest.

References

1. F. K. Mashee, A-R. B. Ali, and M. S. Jasim, *J. Biosci*, **14**, 4777, (2020).
2. M. Ali Al-Anbari, N. Y. Othman, S. Mulahasan, *Innov. Infrastruct. Solut.*, **7**, 225 (2022). <https://doi.org/10.1007/s41062-022-00824-w>
3. H. Emami and A. Zarei, *Remote Sens. Appl. Soc. Environ.*, **23**, 100594 (2021). <https://doi.org/10.1016/j.rsase.2021.100594>.
4. H. Duan, Z. Cao, M. Shen, J. Ma, T. Qi, Y. Liu, and Q. Xu, *National Remote Sensing Bulletin*, **26**, 3 (2022). <https://doi.org/10.11834/jrs.20221301>.
5. H. Q. Hamdi and Z. N. Abdul-Ameer, *J. Phys. Conf. Ser.*, **2114**, 012014 (2021). <https://doi.org/10.1088/1742-6596/2114/1/012014>.
6. R. Hasan, A. Kapoor, R. Singh, and B. K. Yadav, *Environ. Monit. Assess.*, **196**, 1266 (2024). <https://doi.org/10.1007/s10661-024-13315-5>.
7. M. F. Allawi and B. A. Ahmed, *IOP Conf. Ser. Mater. Sci. Eng.*, **757**, 012062 (2020). <https://doi.org/10.1088/1757-899X/757/1/012062>.
8. T. A. Wahhab and F. M. Hassan, *IOP Conf. Ser. Earth Environ. Sci.*, **1088**, 012006 (2022). <https://doi.org/10.1088/1755-1315/1088/1/012006>.
9. K. Dörnhöfer, N. Oppelt, *Ecol. Indic.*, **64**, 105 (2016). <https://doi.org/10.1016/j.ecolind.2015.12.009>.
10. J. G. Liu and P. J. Mason, *Image Processing and GIS for Remote Sensing: Techniques and Applications*, John Wiley & Sons, 2024.
11. K. Kamaruzzaman, S. A. Salleh, and F. Pardi, *Geocarto Int.*, **40**, 2448978 (2025). <https://doi.org/10.1080/10106049.2024.2448978>.
12. J. Song, S. Gao, Y. Zhu, and C. Ma, *BEDJ.*, **3**, 232 (2019). <https://doi.org/10.1080/20964471.2019.1657720>.
13. J. E. Cubillas, E. S. James, B. Li, X. Wang, and L. Zhang, *ISPRS Ann. Photogramm. Remote Sens. Spatial Inf. Sci.*, **X-5-2024**, 33 (2024). <https://doi.org/10.5194/isprs-annals-X-5-2024-33-2024>.
14. S. S. Rwanga and J. M. Ndambuki, *Int. J. Geosci.*, **8**, 611 (2017). <https://doi.org/10.4236/ijg.2017.84033>.
15. X. C. Li, L. L. Liu, and L. K. Huang, *Int. Arch. Photogramm. Remote Sens. Spat. Inf. Sci.*, **XLII-3-W10**, 605, (2020). <https://doi.org/10.5194/isprs-archives-XLII-3-W10-605-2020>.
16. D. Lu and Q. Weng, *Int. J. Remote Sens.*, **28**, 823 (2007). <https://doi.org/10.1080/01431160600746456>.
17. K. Arai, *Int. J. Adv. Comput. Sci. Appl.*, **11**, (2020). <https://doi.org/10.14569/IJACSA.2020.0110904>.
18. P. Lemenkova, *Examples and Counterexamples*, **7**, 100180 (2025). <https://doi.org/10.1016/j.exco.2024.100180>.
19. Z. Lei and T. L. Lei, *Comput. Environ. Urban Syst.*, **113**, 102174 (2024). <https://doi.org/10.1016/j.compenvurbsys.2024.102174>.
20. K. H. Al-Aarajy, A. A. Abbas, and K. Abood, *TEM J.*, **13**, 396 (2024). <https://doi.org/10.18421/TEM131-41>.

21. A. J. Larner, The 2×2 Matrix: Contingency, Confusion, and the Metrics of Binary Classification, Springer Nature, 2024.
22. M. S. Khan, I. Rahman, F. Z. Tanu, M. H. Ovi, and M. S. Mahmud, Int. J. Environ. Clim. Change, **15**, 388 (2025). <https://doi.org/10.9734/ijecc/2025/v15i14700>.
23. G. M. Foody, Remote Sens. Environ., **239**, 111630 (2020). <https://doi.org/10.1016/j.rse.2019.111630>.
24. Y. Zheng, M. Fu, Q. He, Y. He, and J. Huang, Proc. SPIE, **13506**, 1350614 (2025). <https://doi.org/10.1117/12.3057597>.
25. S. Chen, W. Jiang, Z. Zhang, F. Liu, J. Zhang, and H. Ning, Water, **17**, 442 (2025). <https://doi.org/10.3390/w17030442>.
26. A. K. Mohammed and F. K. M. Al Ramahi, Eng. Technol. J., **38**, 66 (2020). <https://doi.org/10.30684/etj.v38i2b.532>.
27. S. S. Saud, S. A. Abdullah, and B. M. Hashim, Iraqi J. Phys., **21**, 66 (2023). <https://doi.org/10.30723/ijp.v21i4.1155>.
28. H. J. Jumaah, M. H. Ameen, G. H. Mohamed, and Q. M. Ajaj, Egypt. J. Remote Sens. Space Sci., **25**, 313 (2022). <https://doi.org/10.1016/j.ejrs.2022.01.013>.
29. H. M. Al-Lami, N. A. Ali, and R. S. Al-Obaidi, Iraqi J. of Sci., **64**, 1030 (2023). <https://doi.org/10.24996/ij.s.2023.64.2.44>.
30. W. H. Hassan and K. Mahdi, Heliyon, **11**, e42090 (2025). <https://doi.org/10.1016/j.heliyon.2025.e42090>.
31. N. S. Ahmed and H. M. Abduljabbar, Ibn Al-Haitham J. Pure Appl. Sci., **36**, 158 (2023). <https://doi.org/10.30526/36.1.2893>.

مراقبة التغيرات لبحيرة الرزازة والمناطق المحيطة بها باستخدام الاستشعار عن بعد ونظم المعلومات الجغرافية

تبارك حيدر محمد حسين¹ وبن عبد الرزاق عباس²

¹ قسم التحسس النائي ونظم المعلومات الجغرافية، كلية العلوم، جامعة بغداد، بغداد، العراق
² وحدة الاستشعار عن بعد، كلية العلوم، جامعة بغداد، بغداد، العراق

الخلاصة:

تُعد بحيرة الرزازة من أهم موارد المياه في العراق، لما لها من قيمة اقتصادية وبيئية كبيرة للبلاد. تشهد البحيرة حاليًا تغيرات بيئية كبيرة وانخفاضًا في منسوب المياه، ويعود ذلك في المقام الأول إلى زيادة التبخر بسبب تغير المناخ وانخفاض تدفق مياه نهر الفرات. لذلك، من المهم رصد التغيرات التي تؤثر على البحيرة باستخدام الاستشعار عن بعد ونظم المعلومات الجغرافية (GIS). تهدف هذه الدراسة إلى تقييم التغيرات البيئية في بحيرة الرزازة من خلال تحليل صور لاندسات 4-5 لعام 2004 وصور لاندسات 8-9 لعامي 2014 و2024. تم الحصول على بيانات المناخ من موقع ناسا للطاقة (2004 و2014) ومحطة الرزازة التابعة لوزارة الزراعة (2024). تم تطبيق التصنيف الخاضع للإشراف باستخدام طريقة أقصى احتمال ومؤشر فرق الماء الطبيعي (NDWI) لتصنيف منطقة الدراسة إلى مياه وتربة ونباتات. حقق التصنيف دقة إجمالية بلغت 94% و97% و98% للأعوام 2004 و2014 و2024 على التوالي. وأشارت النتائج إلى انخفاض ملحوظ في مساحة سطح الماء من 549.22 كيلومترًا مربعًا عام 2004 إلى 189.77 كيلومترًا مربعًا عام 2024، مصحوبًا بتوسع في مساحة التربة وتقلص في الغطاء النباتي. ولوحظ وجود علاقة عكسية قوية ($r = -0.98$) بين ارتفاع درجات الحرارة وانخفاض مساحة سطح الماء، بينما وُجد ارتباط موجب ($r = 0.98$) بين هطول الأمطار ومساحة سطح الماء. وتُبرز الدراسة التدهور المُقلق لبحيرة الرزازة والحاجة الملحة للرصد المُستمر واستراتيجيات إدارة موارد المياه التكميلية.

الكلمات المفتاحية: التصنيف الخاضع للإشراف، التصنيف الغير خاضع للإشراف، نظم المعلومات الجغرافية، تصنيف الاحتمالية القصوى.